Heliyon 6 (2020) e03312

Contents lists available at ScienceDirect

Heliyon

journal homepage: www.cell.com/heliyon

Research article

Effect of temperature on the formation of acrylamide in cocoa beans during drying treatment: An experimental and computational study

Maritza Gil [a,b,c,*], Pablo Ruiz [b,c], Jairo Quijano [b], Julian Londono-Londono [d], Yamilé Jaramillo [a], Vanessa Gallego [a], Frederic Tessier [e], Rafael Notario [f]

[a] Grupo de investigación de Ingeniería de Alimentos GRIAL. Corporación Universitaria Lasallista. Caldas, Antioquia, Colombia
[b] Laboratorio de Fisicoquímica Orgánica, Facultad de Ciencias, Universidad Nacional de Colombia, Sede Medellín AP 3840, Medellín, Colombia
[c] Instituto Tecnológico Metropolitano, Facultad de Ciencias Exactas y Aplicadas, Medellín, Colombia
[d] Sosteligroup – Generation Wellness, Kra. 54B N 37 - 25 Rionegro, Antioquia, Colombia
[e] Faculty of Medicine - University of Lille, 59655 Villeneuve d'Ascq, France
[f] Instituto de Química Física Rocasolano, CSIC, Serrano 119, 28006 Madrid, Spain

ARTICLE INFO

Keywords:
Theoretical computer science
Computational chemistry
Food analysis
Chemical food analysis
Food composition
Elimination reaction
Asparagine
Acrylamide
Drying
Cocoa bean
Reducing sugars

ABSTRACT

The aim of this work was to determine the effect of temperature on the formation of acrylamide in cocoa beans during drying treatment by an experimental and computational study, in order to assess the presence of this neoformed compound from postharvest stage. The computational study was conducted on the reaction between fructose, glyoxal from glucose, and on asparagine at the M06-2X/6-31+G(d,p) level, under cocoa bean drying conditions at 323.15 to 343.15 K. The proposed reaction for acrylamide formation consisted of seven steps, which required to progress a via cyclic transition state of the four members. In addition, step III (decarboxylation) was considered to be the rate-determining step. Glucose followed an E1-like elimination and fructose exhibited an E1cb-like elimination. Computational model showed that the reaction of acrylamide formation was favored by fructose rather than glucose.

The content of reducing sugars, asparagine and acrylamide in fermented and dried cocoa from two subregions of Antioquia-Colombia, as well as roasted cocoa, were evaluated by UHPLC-C-CAD and UHPLC-QqQ. The concentrations of monosaccharides measured at the end of the fermentation and drying process of cocoa nibs showed greater decreases in the levels of fructose as compared to glucose, supporting the main model hypothesis. Acrylamide formation only occurred in Bajo Cauca due to the presence of both precursors and fast drying time (72 h). Finally, it was possible to find the conditions to which acrylamide can be formed from the drying process and not only from roasting, information that can be used for future control strategies.

1. Introduction

Postharvest processes, such as fermentation and drying, are critical for the quality of plant materials derived from coffee and cocoa. These processed grains are highly regarded around the world based on their aroma and flavor. In each of the postharvest processes these products are submitted to, a series of enzymatic and chemical reactions happen. These reactions, are also favored by the initial composition of the cocoa beans, and by the operative conditions such as temperature, relative humidity, and changes in the pH at the time the whole transformation process is carried out. One should notice that these reactions are essential for the development of expected profiles of aroma, flavor, and color, and that this cannot be achieved otherwise during later stages of processing [1, 2]. On the other hand, these processes also lead to the undesired formation of harmful/carcinogenic components such as 2-propenamide, commonly known as acrylamide, due to reactants formations [3, 4, 5, 6]. One of the main reactions under study is the Maillard reaction, which generates acrylamide from free amino acids and by reducing sugars as glucose, which is considered as a more effective precursor than fructose, tagatose, or maltose. Whereas the importance of glyoxal as one of the key sugars fragmentation intermediary was confirmed, controversial results about the order of reactivity are on the conditions of the different studies were conduced [4, 5].

* Corresponding author.
E-mail addresses: ingandreagil@gmail.com, maritzagil@itm.edu.co (M. Gil).

https://doi.org/10.1016/j.heliyon.2020.e03312
Received 14 May 2019; Received in revised form 31 December 2019; Accepted 24 January 2020

The processing of cocoa beans by fermentation is the stage to obtain free amino acids and reducing sugars. Those components form by hydrolysis of peptides and sucrose, respectively. Fructose (FRUC) and glyoxal from glucose (GLY-GLU) play a significant role during the cocoa transformation, because both reactants could correlate to lead to formation of substituted pyrazine and neo-formed compounds, such as acrylamide, during non-enzymatic reactions [4].

The Maillard reaction is expected to occur rapidly during the next stage of industrialization, the roasting, where higher temperatures (above 120 °C) for long time periods are utilized [7, 8, 9]. This reason explains the results of several studies reported on the content of acrylamide and its derivatives in cocoa beans after fermentation, drying and roasting [2, 10, 11, 12]. Usually, the studies do not evaluate the levels of the neo-formed compounds after drying without roasting, likely because the formation of acrylamide is only expected at temperatures higher than those commonly reached by solar (30–50 °C) or artificial (between 50 and 70 °C) drying. Although a recent study showed acrylamide content levels in dried cocoa beans [13], its drying conditions, the composition of cocoa beans and the sample treatment were not reported. These parameters are important in order to carry on the traceability, quality control and to propose mitigation alternatives from this post-harvest stage.

Due to the above, the possibility of acrylamide formation should ideally be controlled at the drying stage, this because asparagine and reducing carbonyls (fructose and glucose) reactants required for Maillard reaction are generated at this stage. That is what happens instead of other mechanisms as the enzymatic pyrolysis of gluten or decarboxylation of asparagine [4, 11, 12, 14, 15, 16, 17].

In this context, the aim of this work was to determine the effect of temperature on the formation of acrylamide in cocoa beans during drying treatment by an experimental and computational study, in order to assess the presence of this neoformed compound from postharvest stage. These will be made to evaluate the feasibility of acrylamide formation from the reaction of fructose or glyoxal from glucose with asparagine at temperatures typical of the drying process of cocoa beans (323.15, 333.15 and 343.15 K) in aqueous phase.

The content of sugars (fructose, glucose and sucrose) and the asparagine in cocoa beans during the postharvest processing steps (fermentation, drying, and roasting) were experimentally measured, as well as the content of acrylamide in dried and roasted cocoa beans to compare the results from a computational study with the real consumption of sugars that may react with asparagine to form acrylamide.

2. Materials and methods

2.1. Computational details

All computational studies were performed with the Gaussian 09 computational package [18] with ab initio methods. The geometric parameters of the reactants, transition states, and products of the reactions studied were optimized at the M06-2X level with the 6-31+G (d,p) basis set [19], in solution phase at 323.15, 333.15 and 343.15 K. Each structure was characterized as a minimum or a saddle point of first order by analytical frequency calculations.

The calculations of the vibrational frequencies in solution were computed using the integral equation formalism variant of the polarizable continuum model (IEFPCM) [20]. To simulate water as the solvent for interaction of the substrates, a dielectric constant of 78.5 at 298 K was used [21]. These values allowed the evaluation of zero-point vibrational energies (ZPEs), and the kinetics and thermochemical parameters of the reaction. However, it neglects any harmonic effects for the calculation of the ZPEs and tends to overestimate them [20, 21]. Some researchers [20, 21, 22] have correlated the harmonic frequencies obtained by theoretical calculations with suitable experimental databases, which allowed the use of an appropriate scale factor [23] of 0.9631 for the zero-point vibrational energies.

Thermal corrections to enthalpy and entropy values were evaluated at three temperatures in the range of 323.15–343.15 K. To calculate enthalpy and entropy values at the mentioned temperatures, differences between the values at those temperatures and 0 K were evaluated according to standard thermodynamics [24].

Intrinsic reaction coordinate (IRC) [25] calculations were performed in order to verify that the localized transition state structures connect with the corresponding minimum stationary points associated with reactants and products.

The bonding characteristics of reactants, transition states, and products were investigated using a population partition technique, the natural bond orbital (NBO) analysis reported by Reed and Weinhold [24, 25]. The NBO formalism provides the values for the atomic natural total charges and also the Wiberg bond indices [26], that are used to follow the progress of the reaction. The bond index as a measure of the bond order and the strength between the bonds developed during the reaction mechanism was defined by Eq. (1) [27]:

$$\delta B_i = \frac{\left(B_i^{TS} - B_i^{R}\right)}{\left(B_i^{P} - B_i^{R}\right)} \tag{1}$$

where R, TS and P refer to reactant, transition state and product, respectively.

The percentage of evolution (% EV) in order to determine the progress of the transformation of any bond involved in the reaction was calculated according Eq. (2):

$$\%EV = 100\delta B_i \tag{2}$$

The average value δB_{av} was calculated as:

$$\delta B_{av} = \frac{1}{n}\sum \delta B_i \tag{3}$$

where n indicates the number of bonds involved in the reaction and allows to measure the advancement of the transition state along the reaction path. The asynchronicity, A, was obtained by Eq. (4):

$$A = \frac{1}{(2n-2)}\sum \frac{\left|\delta B_i - \delta B_{av}\right|}{\delta B_{av}} \tag{4}$$

The synchronicity of the reaction, S_y was calculated as $S_y = 1 - A$.

The NBO analysis was performed using the NBO program [28] implemented in Gaussian 09 computational package [18].

The classical transition state theory (TST) was selected [29, 30] to calculate the kinetic parameters [24]. The rate constant, k(T), was computed using this theory assuming that the transmission coefficient is equal to unity, as expressed by following relation known as the Eyring-Polanyi equation, for the first order reaction (Eq. (5)), and the second one (Eq. (6)):

$$k(T) = \frac{k_B T}{h} e^{\frac{-\Delta G^{\neq}(T)}{RT}} \tag{5}$$

$$k(T) = \left(K_B T/_h\right)\left(RT/_{P^\circ}\right)^{m-1} e^{-\Delta G^{\neq}(T)/_{RT}} \tag{6}$$

where k_B, h, and R are the Boltzmann's constant, the Planck's constant, and the universal gas constant, respectively. $\Delta G^{\neq}$ (T) is the standard-state Gibbs energy of activation, at the absolute temperature T and p° is the standard pressure for a molecular reaction m of order n.

2.2. Chemicals

Standards of fructose (99 %), glucose, and sucrose (99.9 %) were obtained from Sigma Aldrich (North Harrison, USA). Acrylamide standard (99 %) obtained from Ehrenstorfer GmbH, (Augsburgo, Germany). Methanol and acetonitrile used for sugars determination were HPLC

grade Merck (Darmstadt, Germany) and acetonitrile was MS grade to UHPLC-MS/MS. Sep Pak C18 VAc 1cc/50mg was purchased from Waters (NY, USA). Ultrapure water was obtained from a MilliQ water purification system (Millipore Corp., Bedford, MA, USA).

2.3. Plant material

The plant material used in the present study consisted of a mixture of two international clones: CCN-51 (Collection Castro Naranjal), ICS-1 (Imperial College Selection), and two national clones: FEC-2 (Fedecacao El Carmen, Santander) and FLE -2 (Fedecacao Lebrija, Santander), provided by the National Cacao Federation of Colombia - Fedecacao. The four clones were obtained from the production of the secondary harvest of 2017 (March-May) in two subregions of the department of Antioquia, Colombia. Sampling was performed randomly and representatively in different municipalities of the three subregions, as reported by Gil *et al.* (2019) [31].

2.4. Study location

The fermentation study was carried out in three of the main cocoa producing subregions in the department of Antioquia, Colombia. The experimental units were located as follows: Bajo Cauca (BC): La Candelaria farm located on the road that leads from Caucasia to Nechi N 08° 40″6.57'; W 75° 10″9.74′, 76.3 above sea level. Magdalena Medio (M): it was carried out in the Cannes farm located in the Betulia village of Maceo municipality N 06° 31″6.52 '; W 76° 49″4.89'; 1048 m above sea level.

2.5. Fermentation

Fermentation was carried out following the method reported by Gil *et al.* (2019) [31]. The opening of the cobs was carried out 36 h after harvest. The cocoa in slime had a draining time of 4–6 h before weighing in order to obtain the mixture of the clones in the following ratios: CCN-51 (85.9%), ICS-1 (3.0%), FLE-2 (3.2%) and FEC-2 (7.9%). A mass of 112 ± 4.8 kg of the mixture of clones was homogenized into an oak wood drawer by a manual mix, with a stirrer, it was covered with Bijao leaves (Calathea lutea) and finally with a gunnysack. The process was carried out in triplicate for each subregion. In order, to facilitate draining of the mucilage during fermentation, perforations of 0.8 cm were made every 15 cm at the bottom. The turning was done using the same oak wood stirrers used from the beginning. The cocoa in slime was left to rest for 48 h to propitiate the micro-anaerobic conditions at the beginning. After this time, the turning began and it was repeated every 24 h, until the producer in each study zone indicated that it had reached fermentation conditions, those being 132 h in Bajo Cauca and 168 h in Magdalena Medio.

2.6. Natural drying

Fermented cocoa with a moisture content of 0.38 ± 0.01 kg water/kg product (Bajo Cauca) and 0.42 ± 0.02 kg water/kg product (Magdalena Medio) were subjected to solar drying in a constructed marquee with a maximum capacity of 450 kg. The fermented mass was placed on the marquee in a thin layer 5 cm high. The mixture was flipped with a wooden rake every 2 h on the first day every 4 h from the second day until the end of drying (humidity less than 7% wb). The samples were kept in a closed container with silica gel with cobalt indicator, until processing.

During drying, the relative humidity, luminosity, temperature, precipitation hours were recorded and the grain moisture monitoring was measured every morning and afternoon with a Mini GAC PLUS balance. The data was corroborated by the AOAC method (931.04) [32].

2.7. Roasting

The cocoa samples, fermented and dried, were subjected to a roasting process in a convection oven (KitchenAid, USA) at a constant temperature of 288 °C during 10 min. For this process, 100 g of cocoa beans were placed in a stainless-steel tray with perforations to allow uniform air flow in the samples.

2.8. Solid-phase extraction of sugars

Extraction of sucrose, glucose and fructose started with the extraction assisted by ultrasound according to the method reported by Gil *et al.*, (2019b) [33]. First, 20 mg of raw and fermented cotyledons (moisture >10 %) or 10 mg of dried fermented cotyledons (moisture <10 %) were diluted into 600 μL of MilliQ H2O in a microcentrifuge tube of 2 mL. Second, after dilution, the suspension was mixed for 5 min × 3000 rpm. Third, each microcentrifuge tube was carried out in an ultrasound bath (15 min, 25 Hz, 25 °C, 99 %), followed by centrifugation at 10000 rpm during 15 min.

Solid-phase extraction (SPE) cartridges were used to clean-up the samples before UHPLC-C-CAD analysis (UltiMateTM 3000 Dionex, Thermo Scientific, Sunnyvale, CA, USA). 80 μL of supernatant were passed through a cartridge (SePak C18, 1 cc Vac of 50 mg, Waters, USA), previously activated with 1mL methanol and 1 mL of MilliQ water. The extract of sugars was eluted with 720 μL of MilliQ H2O. The eluate was collected and 400 μL were mixed with 200 μL of acetonitrile prior to analysis.

The chromatographic analysis was performed using a micro-HPLC Ultimate 3000 (Thermo Scientific™ Dionex™ Corona™ Veo™). Chromatographic separation was carried out with a Shodex Asahipak NH2 P-50 4E column (5 μm, 150 mm × 4.6 mm) at 30 °C and 10 μL of sample were defined as injection volume. The mobile phase composition was acetonitrile: water 75:25 (v/v) and the flow rate was fixed at 1 mL min^{-1} during 19 min for each sample.

The corona-charged aerosol detector (C-CAD) was set as follows: the nitrogen generator (Peak Scientific, USA) was selected as nebulizing gas, a pressure of 60 ± 7 psi (purity gas ≥99 %), and collection velocity 10 Hz were also fixed for all analyses. The chromatographic data analysis was carried out using a Chromeleon 7.0 software.

2.9. Acrylamide extraction

Extraction of acrylamide was carried out using a QueChERS method reported by De Paola *et al* (2017) with some modifications [34]. In a 50 mL reaction tube, 1 g of cocoa, 10 mL of water MilliQ, and 10 mL of acetonitrile were mixed. The mix was agitated in vortex 30 s at 3000 rpm and taken to -20 °C per 30 min, afterwards a sachet of extraction salt QueChERS AOAC 2007.01 was added, to homogenize the tube was agitated in vortex 3000 rpm per 1 min. The extraction was carried out by ultrasound at 25 °C, per 5 min, 25 Hz frequency and 99 % potency. The supernatant was separated after the centrifugation at 5000 rpm for 15 min at 10 °C. One mL of the supernatant from the acetonitrile phase was added in the tube containing the cleaning salt (150mg MgSO4 + 50mg PSA +50mg GCB), after agitating again for 1 min at 3000 rpm, it was centrifuged at 10000 rpm during 3 min. An aliquot of 500 μl of the extract was transferred to a certificated amber vial for UHPLC-MS provided with an insert and previously filtered through a Nylon membrane of 0.22 μm along with 500μl of mobile phase for its analysis using/by UPLC/MS/MS.

2.10. Chromatographic identification and quantification of the acrylamide

Chromatographic separation and detection of the acrylamide was carried out in a Waters® ACQUITY UPLC® System equipment, when passing 5 μL of the extract kept at 10 °C, through a column CSH ACQUITY UPLC CSH™ C18 1.7 μm (2.1 × 100 mm) at 30 °C, with a mobile phase composed of water at 0,1 % formic acid (A) and acetonitrile (B) in a ratio

95:5 without elution gradient and a flow of 0.3 mL/min for 5 min. Detection was carried out in a Waters® Xevo® Triple Quadrupole Detector (TQD) equipment and a source of ionization by electro spray– ESI in positive mode using N_2 as solvent in a flow of 1000 L/h and desolvation temperature of 500 °C and capillary voltage of 3 kV. According to the conditions of voltage and energy of collision the ratio mass/charge (m/z) of the precursor ion was 71.7498 and the first ion product 43.8367 at 22 v and 12 of collision energy, the second ion product was 54.8488 with the same voltage and a collision energy of 10.

Quantification was carried out with external standard. 1 mg of the standard of acrylamide in an amber vial of 1.5 mL was dissolved in 1000 μL of acetonitrile to obtain a final concentration of 1000 mg/mL. The mix considered as stock solution was homogenized at 3000 rpm for 30 s, which can be stored four weeks maximum in amber containers, at -20 °C. Concentrations prepared from the stock solution comprised the range from 10.0, 20.0, 30.0, 50.0 100.0, 300.0 to 500.0 μg/L, according to the limits of detection previously verified. For the matrix effect correction, it was necessary to add 300 μL of the extract obtained from the non-fermented cocoa extraction (acrylamide free) with the procedure previously described and the solution of every concentration were adjusted to 1000 μL with acetonitrile.

2.11. Statistical analysis

The statistical significance for differences among the influence of the temperatures by activation energies kinetic constants of the rate-determining step was evaluated by one-way Analysis of Variance (ANOVA). Comparison of means were carried out to analyze by Tukey test ($p < 0.05$). All analyzes were performed using the statistical software R Studio (Version 0.98.1103 GNU Affero General Public License).

3. Results and discussion

3.1. Reaction mechanism and determination of kinetic parameters

The proposed pathway for acrylamide formation from the carbonyl such as fructose (hydrolyzed sucrose components), and the glyoxal formed from glucose, in presence of asparagine at temperatures of approximately 323.15 K during the drying process, corresponds to a seven-step mechanism.

The first step consisted of an addition reaction resulting from the nucleophilic attack of the amino group of the asparagine on the aldo or keto group from glucose and fructose, respectively, via a four-membered cyclic transition state, TS_1, resulting in the first intermediate (INT I). The second step was a water elimination where the hydrogen atom (β) of the NH present in the first intermediate migrates toward the oxygen atom of the next hydroxyl group resulting in an E1c-like elimination reaction where the abstraction of the proton was favored following the expulsion of the leaving group (second intermediate – INT II). The above steps preceded the rate-determining stage corresponding to the decarboxylation process by a *Syn* elimination of the second intermediate leading to a loss of CO_2 and the formation of the third intermediate (INT III).

The determining step was followed by a hydrolysis, which occurs in two steps. An addition of water (step IV) to the double bond formed between N and C and the re-arrangement and breaking of the fourth intermediate (INT IV) via a four-membered cyclic transition state, TS_5. This rupture gave rise to the more reactive intermediate for the formation of acrylamide, which is the 3-amino propanamide (INT V) and a by-product, which differs according to the precursor sugar, if it comes from FRUC was (2,3,4,5-tetrahydroxy pentanoic acid) and from GLY-GLU was (3,4,5,6-tetrahydroxy-2-oxo-7-hexanal).

From INT V, the two final stages were common to the two precursors from sugars. Step VI was a displacement of the charge on the two major functional groups caused by a tautomerism that consisted of a translation of the adjacent hydrogen from the carboxyl group to the amino group (δ^+), resulting in the formation of ammonia, which will be removed from the molecule by a β-elimination (step VII) to culminate with the formation of the resonant structure of acrylamide [35]. The reaction mechanism for glucose is shown in Figure 1 and fructose undergoes a similar pathway.

Sucrose follows the same reaction pathway, with the exception that it first undergoes hydrolysis to convert into glucose and fructose and continues with the transformation described above.

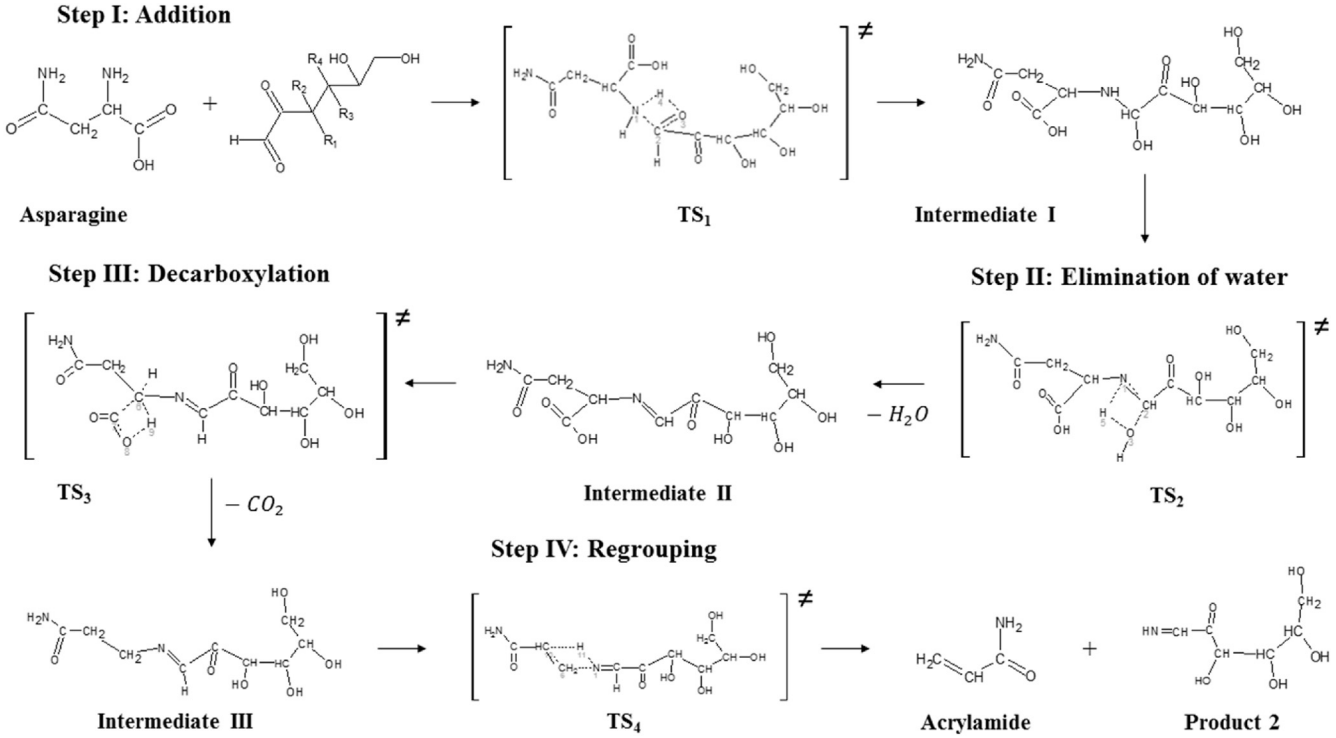

Figure 1. Mechanism of formation of acrylamide from the reaction between asparagine and glyoxal formed from glucose.

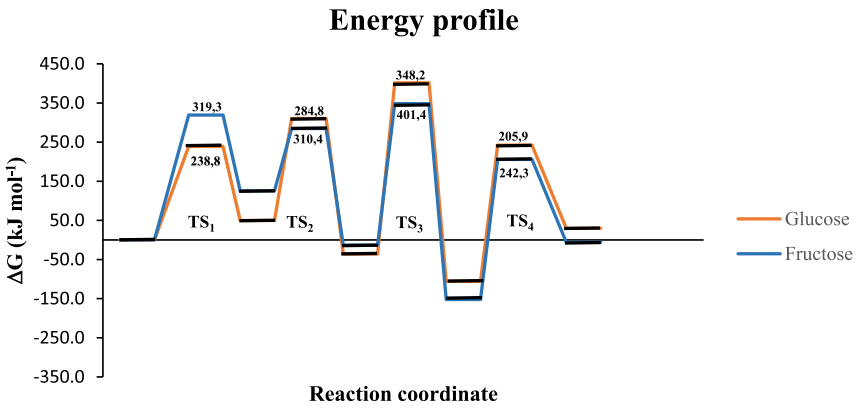

Figure 2. Gibbs free energy profile at 333.15 K evaluated at M06-2X/6-31+G(d,p) level for the molecular thermal formation of acrylamide from GLY-GLU and FRUC.

The transition states showed only one imaginary vibrational frequency in aqueous phase in order to lead the products with their optimized geometries resulting from the proposed mechanism for the formation of acrylamide. Calculated imaginary frequencies for the different steps were: I (1491.4i; 1630.4i), II (1381.2i; 1508.5i), III (1824.4i; 1732.1i), IV (1412.7i; 1732.1i) and V (1519.4i; 1499.0i), for GLY-GLU and FRUC, respectively. Imaginary vibrational frequencies are the same for both reactants in steps VI (1601.5i) and VII (414.5i).

Figure 2 illustrates the rate-determining step into the Gibbs energy profiles for acrylamide formation from GLY-GLU and FRUC with asparagine in aqueous phase at 333.15 K, respectively. Notice the same behavior through the whole temperature range except for the first step that required more energy to concert the addition of FRUC to the asparagine compared with the GLY-GLU.

As mentioned above, the third stage was the rate-determining step for all the mechanism evaluated. The Gibbs free energy in aqueous phase for GLY-GLU, at 333.15 K, was 298.4 kJ/mol and for FRUC 274.0 kJ/mol (Table 1).

In general, the differences between the height of the barriers in the energy profiles (24.3 ± 0.3 kJ/mol) and activation energies (13.2 kJ/mol) permit to infer that the fructose requires less energy and is faster than glyoxal to convert the reactants to the products during the rate-determining step along the range of studied temperatures (Table 1). In order to understand this behavior, the magnitude of $\Delta H^{\neq}$ and $\Delta S^{\neq}$ parameters confirm that the position of the atoms involved in the transition state structure do not correspond to their position in the ground state. A higher value of $\Delta H^{\neq}$ for GLY-GLU (296.4 kJ/mol) than for FRUC (283.2 kJ/mol) indicates that more energy is required for bond reorganization to form the acrylamide, and $\Delta S^{\neq}$ allowed measuring the degree of organization resulting from the formation of the active complex [36].

The overall process was exergonic, with reaction Gibbs free energy of -37.3 and -29.0 kJ/mol in aqueous phase for GLY-GLU and FRUC,

Table 1. Calculated activation enthalpies, entropies, Gibbs free energies and kinetic constant for the molecular formation reactions of acrylamide from glucose and fructose with asparagine, in gas phase at 298,15 K and in aqueous phase from 323.15 K, 333.15 K, 343.15 K and 393.15 K.

Step	Glucose				Fructose			
	$\Delta H^{\neq}$ (kJ/mol)	$\Delta S^{\neq}$ (J/mol*K)	$\Delta G^{\neq}$ (kJ/mol)	k (s^{-1})	$\Delta H^{\neq}$ (kJ/mol)	$\Delta S^{\neq}$ (J/mol*K)	$\Delta G^{\neq}$ (kJ/mol)	k (s^{-1})
Gas phase at 298.15 K								
I	169.5	-114.9	224.1	7.9×10^{-26}	234.8	-143.2	302.8	1.2×10^{-39}
II	327.5	-10.3	332.4	3.3×10^{-46}	270.9	-7.7	274.5	4.7×10^{-36}
III	390.7	-0.6	391.0	1.8×10^{-56}	377.2	11.3	371.8	4.0×10^{-53}
IV	336.3	-31.0	351.1	1.1×10^{-47}	195.0	-29.1	208.8	1.5×10^{-24}
Aqueous phase at 323.15 K								
I	175.4	-119.4	236.9	5.5×10^{-23}	245.3	-143.8	319.4	4.2×10^{-38}
II	307.5	-5.5	310.4	4.6×10^{-38}	276.4	-16.3	284.8	6.1×10^{-34}
III	398.6	-5.2	401.3	9.2×10^{-53}	353.8	10.9	348.2	3.5×10^{-44}
IV	223.0	-36.3	241.7	5.8×10^{-27}	192.4	-26.2	205.9	3.5×10^{-21}
Aqueous phase at 333.15 K								
I	175.4	-119.4	238.8	6.9×10^{-24}	245.2	-144.0	319.3	1.6×10^{-36}
II	307.5	-5.6	310.4	1.5×10^{-36}	276.4	-16.4	284.8	6.1×10^{-34}
III	398.6	-5.2	401.4	8.2×10^{-51}	353.8	11.0	348.2	3.5×10^{-44}
IV	222.9	-36.6	242.3	7.1×10^{-26}	192.3	-26.3	205.9	3.5×10^{-21}
Aqueous phase at 343.15 K								
I	175.3	-119.5	240.7	4.6×10^{-23}	245.2	-144.1	319.3	4.9×10^{-35}
II	307.5	-5.6	310.5	3.8×10^{-35}	276.3	-16.6	284.8	6.1×10^{-34}
III	398.6	-5.1	401.4	5.6×10^{-49}	353.9	11.1	348.2	3.5×10^{-44}
IV	222.8	-36.8	242.9	7.7×10^{-25}	192.3	-26.4	205.9	3.5×10^{-21}
Aqueous phase at 393.15 K								
I	178.3	-119.7	250.2	1.5×10^{-19}	250.6	-144.5	335.4	7.1×10^{-31}
II	308.7	-6.0	311.0	2.3×10^{-27}	279.4	-17.3	286.7	6.6×10^{-26}
III	398.6	-5.0	401.8	3.3×10^{-41}	351.5	11.6	346.9	6.6×10^{-34}
IV	228.1	-37.6	245.8	1.8×10^{-20}	195.1	-26.8	208.8	1.5×10^{-15}

Table 2. Wiberg bond indexes (Bi) of reactans (R). transition state (TS) and products (P) for the four steps to the molecular thermal formation of acrylamide from glucose and fructose with asparagine.

Step I - Glucose					Step I – Fructose				
	N_1-C_2	N_1-H_4	H_4-O_3	C_2-O_3		N_{10}-C_4	N_{10}-H_{15}	H_{15}-O_5	C_4-O_5
B_i^R	0.000	0.809	0.000	1.869	B_i^R	0.000	0.809	0.000	1.745
B_i^{TS}	0.872	0.406	0.279	1.075	B_i^{TS}	0.870	0.379	0.307	1.005
B_i^P	1.004	0.008	0.705	0.933	B_i^P	0.998	0.001	0.698	0.891
%EV	86.82	50.24	39.58	84.89	%EV	87.13	53.23	43.97	86.69
	$\delta B_{av} = 0.65$		$Sy = 0.79$			$\delta B_{av} = 0.68$		$Sy = 0.81$	
Step II - Glucose					Step II – Fructose				
	N_1-H_{15}	H_5-O_3	N_1-C_2	C_2-O_3		N_{10}-H_{14}	H_{14}-O_5	N_{10}-C_4	C_4-O_5
B_i^R	0.755	0.001	1.004	0.934	B_i^R	0.768	0.001	0.998	0.891
B_i^{TS}	0.275	0.382	1.226	0.645	B_i^{TS}	0.261	0.378	1.163	0.630
B_i^P	0.000	0.754	1.896	0.000	B_i^P	0.000	0.754	1.860	0.000
%EV	63.54	50.60	24.89	30.90	%EV	66.05	50.11	19.07	29.26
	$\delta B_{av} = 0.42$		$Sy = 0.77$			$\delta B_{av} = 0.41$		$Sy = 0.73$	
Step III - Glucose					Step III – Fructose				
	C_6-C_7	C_6-H_9	O_8-H_9	C_7-O_8		C_6-C_7	C_6-H_{16}	O_9-H_{16}	C_7-O_9
B_i^R	0.930	0.019	0.693	1.061	B_i^R	0.941	0.001	0.620	1.118
B_i^{TS}	0.189	0.199	0.419	1.353	B_i^{TS}	0.522	0.312	0.217	1.449
B_i^P	0.000	0.881	0.000	1.883	B_i^P	0.000	0.903	0.000	1.883
%EV	79.67	20.84	39.50	35.54	%EV	44.50	34.46	65.01	43.24
	$\delta B_{av} = 0.44$		$Sy = 0.73$			$\delta B_{av} = 0.47$		$Sy = 0.87$	
Step IV - Glucose					Step IV – Fructose				
	C_{10}-H_{11}	H_{11}-N_1	C_6-N_1	C_6-C_{10}		C_5-H_{12}	H_{12}-N_{10}	C_6-N_{10}	C_5-C_6
B_i^R	0.887	0.001	0.100	0.997	B_i^R	0.879	0.001	0.991	0.996
B_i^{TS}	0.241	0.505	0.900	1.029	B_i^{TS}	0.002	0.756	0.593	1.296
B_i^P	0.000	0.832	0.000	1.945	B_i^P	0.000	0.813	0.000	1.945
%EV	72.86	60.59	9.99	3.45	%EV	99.73	92.98	40.10	31.53
	$\delta B_{av} = 0.37$		$Sy = 0.46$			$\delta B_{av} = 0.66$		$Sy = 0.69$	

% EV: percentage of the evolution of a bond; $\delta B_{av:}$ average value; synchronicity.
See numering in Figure 2.

Table 3. NBO charges calculate at HF/6-31G (d) level. at the atoms involve in the reaction center for the four steps to the molecular thermal formation of acrylamide from glucose and fructose with asparagine in aqueous phase.

Step I - Glucose					Step I - Fructose				
	N_1	H_4	C_2	O_3		N_{10}	H_{15}	C_4	O_5
R	-0.952	0.412	0.470	-0.619	*R*	-0.952	0.412	0.675	-0.691
TS_1	-0.781	0.556	0.282	-0.973	TS_1	-0.788	0.551	0.477	-0.990
$P_{intermediaryI}$	-0.776	0.514	0.281	-0.826	$P_{intermediaryI}$	-0.801	0.516	0.474	-0.857
Step II - Glucose					Step II – Fructose				
	N_1	H_{15}	C_2	O_3		N_{10}	H_{14}	C_4	O_5
R	-0.776	0.430	0.281	-0.826	*R*	-0.801	-0.801	0.474	-0.857
TS_2	-0.933	0.577	0.273	-0.850	TS_2	-0.957	0.587	0.492	-0.892
$P_{intermediaryII}$	-0.487		0.102		$P_{intermediaryII}$	-0.603		0.374	
P_{water}		0.494		-0.988	P_{water}		0.494		-0.988
Step III - Glucose					Step III – Fructose				
	C_6	C_7	O_8	H_9		C_6	C_7	O_9	H_{16}
R	-0.130	1.020	-0.777	0.529	*R*	-0.150	1.013	-0.801	0.550
TS_3	-0.376	1.142	-0.793	0.555	TS_3	-0.355	1.111	-0.804	0.566
$P_{intermediaryIII}$	-0.222			0.242	$P_{intermediaryIII}$	-0.210			0.230
P_{CO2}		1.277	-0.638		P_{CO2}		1.277	-0.638	
Step IV - Glucose					Step IV – Fructose				
	C_{10}	H_{11}	C_6	N_1		C_5	H_{12}	C_6	N_{10}
R	-0.538	0.257	-0.222	-0.452	*R*	-0.532	0.245	-0.210	-0.578
TS_4	-0.675	0.457	-0.191	-0.501	TS_4	-0.669	0.431	-0.120	-0.639
$P_{acrylamide}$	-0.365		-0.297		$P_{acrylamide}$	-0.365		-0.297	
$P_{product2}$		0.374		-0.652	$P_{product2}$		0.376		-0.732

respectively. Even though, the steps I, IV, and VI were endergonic for both reactants and the step V was endergonic for GLY-GLU, the total energy of the reaction allowed carrying out the reaction through the whole pathway. The results indicate that the formation of acrylamide is thermodynamically favorable at the studied temperatures and it could be possible to find this neo-formed compound during the drying process and not only during the roasting process as has been previously reported [12, 37, 38].

In order to explain the progression of the reactants through the proposed reaction for the formation of acrylamide from asparagine and fructose or glyoxal from glucose (Figure 1), it was necessary to analyze the development of the bond and the charges on the involved elements by the Natural Bond Orbital (NBO) calculations [26]. The results are shown in Table 2.

During the decarboxylation, the receptor carbon C6 in the fructose was slightly less negative than in the GLY-GLU and this enhanced reactivity may be due to the inductive –I effect of the C6 receptor atom (i.e., the electron withdrawing inductive effect brought about C-H bond polarization) which makes the C-O bond cleavage easier. The -I effect could be greater in fructose because the substituent group is –CHOH next to the C6-N=C instead of the –H in glyoxal. This may be derived from the ability of the hydroxyl group to stabilize itself by solvation and the effect of the N=C group may be higher, in order to mark the difference of electronegativity [39].

With respect to the percentage of advance of the reaction (% EV), in the first step the higher evolution was 80 % for the bond formed between the N atom of the asparagine and the C atom of the carbonyl. The calculated synchronicity S_y values were 0.89 (GLY-GLU) and 0.87 (FRUC). Although the activation energy of this first step is greater with the fructose-acrylamide complex than with glyoxal from glucose as mentioned above, it is evident that the formation of N-glycosyl asparagine progresses almost entirely under the temperature conditions studied.

During the progress of the reaction in order to obtain the Schiff base involved in TS the double C=N presents a lower 22 % of advance, and the breaking of the C-O, opposite to the attraction of the H from the O atom, presents a 51.8 % (fructose) or 53.8 % (glucose) of advance. These results agreed with the elimination reaction E1c-like observed for this step. Glyoxal from glucose and fructose had the same behavior.

GLY-GLU presented a % EV of the bond during step III of 53.6 % obeying possibly to the type of the elimination reaction E1-like because the expulsion of the leaving group occurred first, and this path was corroborated by IRC calculations that allowed to verify the connections between the localized transition structures with respective reactants and products. On the other hand, fructose had the highest progression on cleavage of the bond O-H (61.1%) and the abstraction of the proton was favored at same time that the breaking of the bond C6-C7, a mechanism that corresponds to an elimination E1cb. This last value coincides with the mechanism expected for the decarboxylation, where higher energy is required for the formation of the charge on the C atom receptor of the H. The TS of the fructose had a greater development of the bond corresponded to the addition to the C6 of the H atom from O-H group, instead of the cleavage bond of C6-C7 to form the carbanion, which is the rate-determining step expected for the decarboxylation reaction [40]. The rate-determining step had not differences, between the synchronicity for both reactants (0.85).

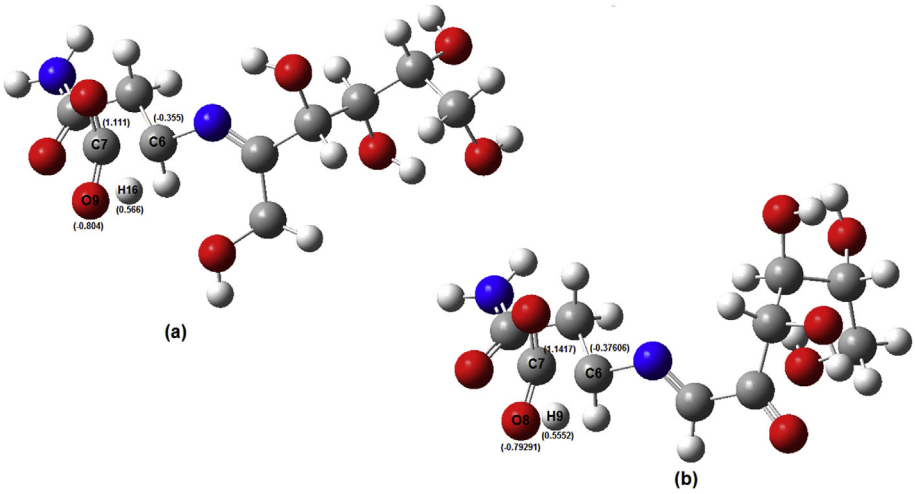

Figure 3. Charges NBO at the atoms involved in the reaction center of the optimized structures of the transition state for the rate-determining step of the molecular formation of acrylamide from the reaction between fructose (a) and glyoxal from glucose (b) with the asparagine in aqueous phase, calculated at M06-2X/6-31+G(d,p) level.

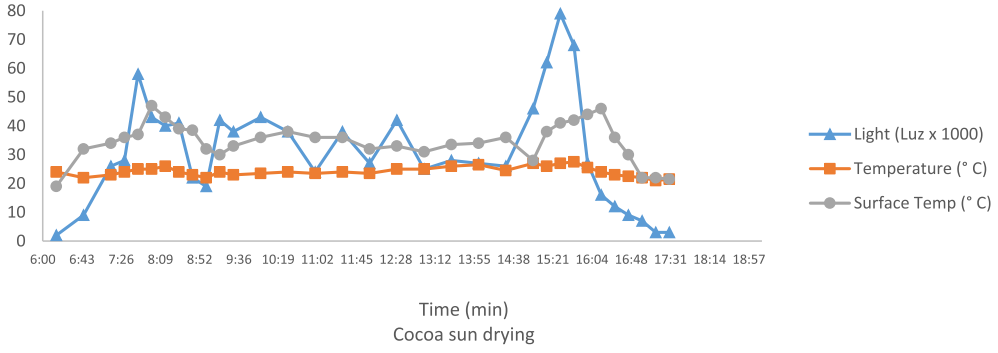

Figure 4. Temperature of the environmental and surface of drying (°C) and intensity of light (Lux x 1000) in the range of 6:15 a.m to 5:30 p.m.

Whereas the bond with most advanced cleavage was the O-H in glucose in order to form the CO_2.

In general, the synchronicities varied between 0.74 and 0.90 for fructose, indicated that the mechanism is a slightly asynchronous process. In the same way, S_y for glucose was in the range of 0.73 and 0.89. This behavior shows that the implicated bond in the reaction center was not broken or formed to the same extent in the TS. The exception for both reactants was the step V ($S_y \sim 0.50$), result oriented to an asynchronous movement.

The calculated δB_{av} values indicate the character of the transition states. These values for GLY-GLU and FRUC were less than 0.50 for steps II, III, V, and VI, indicating an "early" character, nearer to the reactants than to the products. Opposite results were observed for steps I and IV, mechanisms of reaction that exhibited "late" character.

Table 3 presents the natural atomic charges at the atoms involved through each step of the reaction mechanism. During the decarboxylation, the enhanced reactivity of the receptor carbon C6 initiator of the carbanion formation was shown more viable for GLY-GLU. This is based on the slight increase in charge on the C6-glyoxal (-0.388) compared with fructose (-0.378). The above differences maybe explained based on the decreased reactivity when the carbanion was stabilized by inductive effect from the closeness of the -N=C-R1R2 ($R2_{fructose}$: CH-OH).

The atomic charge was another indicator that suggests an asynchronous character during the rate-determining step (step III). An asynchronous charge distribution occurs between C_α (C6) and C_β (C7) atoms during the transition structure that results in a decarboxylation reaction (negatively charged C_α and positively charged C_β) for both reactants. The difference in the polarity between C6-C7 bond could propitiate a faster reaction (see Figure 3) [39].

3.2. Effect of the temperature

The reactants are not the only cause to improve the kinetic constant for the molecular formation of acrylamide. The variation of temperatures can also have a direct influence that presented significant differences ($p < 0.05$) between the evaluated activation kinetic energy constants of the rate-determining step for the drying and roasting temperatures in aqueous phase. These constants were 6.4×10^{-29} s^{-1} and 5.4×10^{-24} s^{-1} at 393.15 K during roasting for GLY-GLU and FRUC, respectively. These constants were faster than the obtained for drying temperatures in the same phase, shown in Table 1.

There are evidences that high temperatures accelerate the activation of the initial complex reducing sugar – amino acid, in general terms, the value of its temperature coefficient, Q10 (in the range of 0–70 °C), varies from 2 to 3; i.e. for every 10 °C of increase, the speed fold two or three times. In this case, the velocity constants ratios of 333.15/323.15 K and 343.15/333.15 K were calculated as 3.65 and 3.45 for fructose, and 2.47 and 2.41 for glucose, respectively. This relation increased during rate-determining step over 20 for both reactants [41].

In order to compare the drying and roasting processes, a similar computational study in aqueous phase was conducted at 393.15 K, temperature used for the roasting process. The results showed that the increasing of temperature presented significant differences ($p < 0.05$) for changing in the energy of reaction in the rate-determining step for the drying temperatures compare with roasting temperatures. Opposite to the comparison between 323.15 to 333.15 K. Compared with the reaction Gibbs free energy profile shown in Figure 2, the variations were between 8 and 10%. It should be noted that the free energy for glucose increased and for fructose decreased.

The supposition that the formation of acrylamide occurs only during the roasting process could be due to that the temperature around the cocoa beans during the drying is expected to be less than 300 ± 5 K. In contrast, Figure 4 shows that the profile of the recorded environmental temperatures were between 293.15 and 303.15 K, but raised on the surface of drying, because of heat transfer by conduction from the material to the cocoa beans. The intensity of the light (Lux_x 1000) produced higher drying temperatures that ranged from 293.15 and 353.15 K. The temperatures evaluated in this study fall within this range and therefore corroborate that drying process is the probable stage for the production of acrylamide (see Figure 4).

Calculated values of the activation parameters E_a and A-factor and the rate expression for the thermal acrylamide formation in aqueous phase are collected in Table 4, and the data could be fitted to the Arrhenius equation for both reactants. The proposed reaction steps have been described previously for the reaction between the studied sugars with the asparagine [3, 5, 42]. Even though results from the current computational model are not completely conclusive, the kinetic parameters provide information that is not currently available for this mechanism from previous experiments at proposed temperatures.

Kinetic rate constants for the acrylamide formation from the reaction of the studied monosaccharides with asparagine were calculated in aqueous phase at 323.15, 333.15 and 343.15 K. The Arrhenius plot leads to an equation of first order (see Figure 5) in which the plots are almost parallel and superimposable with a difference of 12 % for FRUC over GLY-GLU.

3.3. Precursors of acrylamide

Asparagine, necessary reactant for the formation of acrylamide, was only detected at the end of fermentation in Bajo Cauca (533.0 ± 11.5 mg/

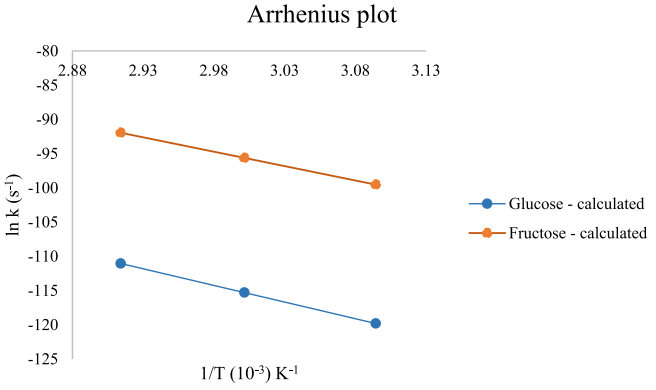

Figure 5. Arrhenius plot at 323.15, 333.15 and 343.15 K for the molecular thermal formation of acrylamide from glyoxal formed from glucose (GLY-GLU) and fructose (FRUC) with asparagine. Theoretical kinetic constants were determined in this work at M06-2X/6-31+G(d,p) level.

Table 4. Computational rate expression, activation energies and A-factors for the thermal formation of acrylamide from glucose and fructose with asparagine calculated in the range from 323.15 at 343.15 K.

Parameter	Calculated	
	Glucose	Fructose
Rate expression, (s^{-1})	$\ln k = (30.57 \pm 8.7 \times 10^{-3})$ - (48.59 ± 2.9) T^{-1} (kJ mol^{-1})	$\ln k = (30.57 \pm 8.7 \times 10^{-3})$ - $(42{,}041 \pm 2.9)$ T^{-1} (kJ mol^{-1})
A (s^{-1})	1.89×10^{13}	1.89×10^{13}
Ea $_{(kJ\ mol)}^{-1}$	404.0	349.5

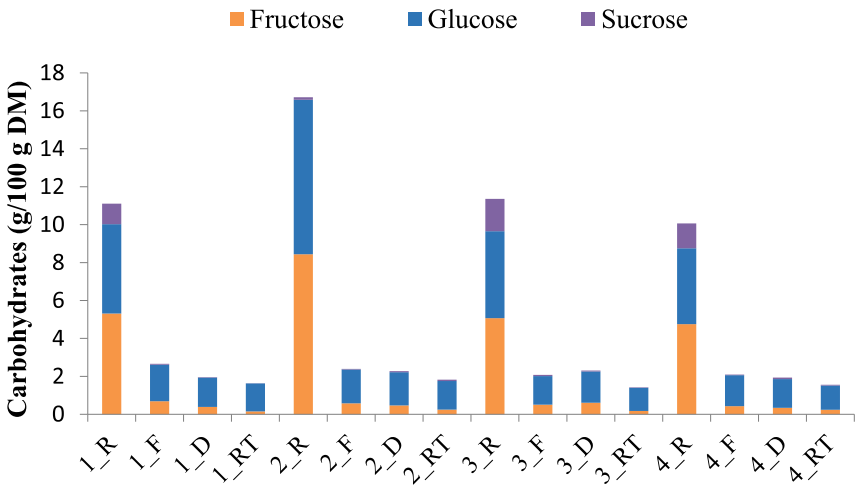

Figure 6. Sugar content through post-harvest of cocoa bean in Bajo Cauca and Magdalena Medio. R: Raw, F: Fermented, D: Dried, DM: Dry.

kg). As regards Magdalena Medio, the quantity was below of the Limit of Detection (LOD).

As is shown above in Table 1, the rate-determining step for FRUC is faster than the one for GLY-GLU, this result coincides with the content of sugars in cocoa beans during the post-harvest process (raw, fermented and dried) (see Figure 6).

The concentration of the sugars in the cocoa beans of Bajo Cauca decreases during the fermentation in the order sucrose (96.8 % w/w) > glucose (92.3 % w/w) > fructose (77.2 % w/w). On the other hand, in Magdalena Medio the sucrose and fructose decrease 99.4% and 63.1% respectively and the glucose increase 77.2%. Sucrose is explained because the hydrolysis reaction is easier under the condition of the pH, temperatures and presence of the enzymes during the fermentation [2]. On the other hand, the concentration of fructose (from 5.9 ± 0.7 to 0.2 ± 0.04 g/100 g_{DM} - 96.6 %) decreased more than glucose during the three stages (from 5.4 ± 0.8 to 1.4 ± 0.01 g/100 g_{DM} - 74.4 %). It matches the computational findings.

During fermentation of the cocoa beans, fructose could be more active in other pathways to form precursors of flavor [4]. In the same way, through the drying and roasting, fructose was more reactive than glucose, even though the fructose was at lower levels after fermentation of the raw cocoa beans (see Figure 6). This behavior of decreasing and favoring greater reactivity of fructose instead of glucose during the decarboxylation and re-arrangement in order to form the acrylamide under the evaluated temperatures could be due to the high correlation of the fructose to produce substituted pyrazines during cocoa fermentation, and to continue the acrylamide production under conditions of roasting according to previous studies [4, 43] and drying as these results have shown.

3.4. Acrylamide content in fermented and dried cocoa samples

From the computational study, it is clear that the formation of acrylamide is influenced by the reactants and the temperature, as has been demonstrated in other studies for other raw materials.

Although a recent study showed the presence of acrylamide in dried cocoa beans, it is necessary to know the conditions that allow future control during post-harvest processes such as drying [13].

The content of acrylamide detected in the dry cocoa of Bajo Cauca through the natural drying (0.079 ± 0.034 mg/kg) allowed to verify that the formation of this thermal contaminant can occur by drying and not only in the processing stages during industrialization as it was expected, i.e. acrylamide content in chocolate 4.90 mg/kg [44]. This confirms the thermochemical viability shown in the computational model at the minimum study temperature (323.15 K). The possible causes could be due to the high temperatures on the surface of the marquee reached during the process (Figure 4) and the short drying time (72 h) compared to drying time required in Magdalena Medio (182 h), where no acrylamide was detected. In this respect, acrylamide was not formed during solar drying in Magdalena Medio due to the low concentration of precursors at the end of fermentation.

In general, the values of acrylamide in cocoa were between 45-113 μg/kg and close to those reported by Raters & Matissek (2018), since the unroasted cocoa beans were between 50 and 80 μg/kg [13].

Under conditions of industrialization, such as roasting, the formation of acrylamide is favored by high temperatures. In the case of Bajo Cauca, the acrylamide value increased to 0.2606 ± 0.015 mg/kg (76 %), and in Magdalena Medio the formation of acrylamide was favored because asparagine was detected at the end of solar drying (5.040 mg/kg) and added to the high temperatures, an acrylamide value of 0.090 ± 0.078 mg/kg was quantified.

The results obtained in the cocoa samples are relevant since they are below the tolerable dose established by the European Food Safety Authority (EFSA), within which experts have found that acrylamide can cause a small tumor incidence (BMDL10 of 0.17mg/kg_{wb}/day) or adverse effects such as prenatal and postnatal neurological development (BMDL10 of 0.43 mg/kg_{wb}/day) [45].

Although to date there are no reference limits and mitigation measures of acrylamide in samples of cocoa and its by-products in the Regulation (UE) 2017/2158 that came into force in April 2018, these are results that in the future can be taken into account within this regulation [46].

4. Conclusions

The current theoretical study evaluated the formation of acrylamide by the well know Maillard reaction pathway between fructose or glyoxal from glucose and asparagine, under the simulated conditions of drying of cocoa beans from 323.15 to 343.15 K. Previously, the formation of acrylamide was expected to occur rapidly only at the higher temperatures that are used during the roasting of cocoa beans. The current study, however, shows that the overall process of Maillard reaction is exergonic and is therefore thermodynamically favorable even at lower temperatures used in the cocoa bean drying process.

The proposed reaction mechanism included seven steps including reactions of addition, water elimination, decarboxylation, hydrolysis, arrangement and elimination of ammonia. The rate-determining step is the decarboxylation process, which was more favorable with fructose relative to glucose. However, the first two stages (addition and water

elimination) appear more advantageous for glyoxal from glucose. The Gibbs free energies for the molecular formation did not have significant change between the drying and roasting processes.

The decarboxylation step for glyoxal from glucose and fructose follow an elimination reaction type E1-like and E1c-like, respectively, which could affect the energy barrier required to overcome the step. The mechanistic aspects that coincided for both reactants are, 1) the slightly asynchronous reaction, 2) the cyclic transition state formed by four atoms with an "early" character, and 3) the reaction rate is favored by higher temperature, especially for the roasting instead of the drying process. There were significant differences between both processes.

The result obtained on the higher reactivity of fructose instead of the glyoxal from glucose coincided with the increased consumption of fructose during the stages of postharvest (fermentation and drying) under temperatures that may reach the same studied values, either by the use of sunlight or artificial drying.

Thermochemical data obtained from this study may be useful for improving the cocoa bean drying process, in order to control the formation of acrylamide that is known for its harmful effects on human health.

Declarations

Author contribution statement

Maritza Gil: Conceived and designed the experiments; Performed the experiments; Analyzed and interpreted the data; Contributed reagents, materials, analysis tools or data; Wrote the paper.

Pablo Ruiz, Yamile Jaramillo: Performed the experiments; Analyzed and interpreted the data; Wrote the paper.

Jairo Quijano: Analyzed and interpreted the data; Contributed reagents, materials, analysis tools or data.

Julian Londono-Londono: Conceived and designed the experiments.

Vanessa Gallego: Analyzed and interpreted the data; Wrote the paper.

Frédéric Tessier: Contributed reagents, materials, analysis tools or data.

Rafael Notario: Contributed reagents, materials, analysis tools or data; Wrote the paper.

Funding statement

This work was supported by Government of Antioquia through Science and Technology Fund (General System of Royalties), Antioquia-Colombia, contract 4600003895. It was also supported by Colciencias-Colfuturo and Universidad Nacional de Colombia, scholarship No. 647-2015.

Competing interest statement

The authors declare no conflict of interest.

Additional information

Supplementary content related to this article has been published online at https://doi.org/10.1016/j.heliyon.2020.e03312.

References

[1] R. Saltini, R. Akkerman, S. Frosch, Optimizing chocolate production through traceability: a review of the influence of farming practices on cocoa bean quality, Food Contr. 29 (2013) 167–187.

[2] J.E. Kongor, M. Hinneh, D. Van de Walle, E.O. Afoakwa, P. Boeckx, K. Dewettinck, Factors influencing quality variation in cocoa (Theobroma cacao) bean flavour profile - a review, Food Res. Int. 82 (2016) 44–52.

[3] R.H. Stadler, F. Robert, S. Riediker, N. Varga, T. Davidek, S. Devaud, T. Goldmann, J. Hau, I. Blank, In-depth mechanistic study on the formation of acrylamide and other vinylogous compounds by the maillard reaction, J. Agric. Food Chem. 52 (2004) 5550–5558.

[4] G. Koutsidis, A. De La Fuente, C. Dimitriou, A. Kakoulli, B.L. Wedzicha, D.S. Mottram, Acrylamide and pyrazine formation in model systems containing asparagine, J. Agric. Food Chem. 56 (2008) 6105–6112.

[5] W.L. Claeys, K. De Vleeschouwer, M.E. Hendrickx, Kinetics of acrylamide formation and elimination during heating of an asparagine-sugar model system, J. Agric. Food Chem. 53 (2005) 9999–10005.

[6] S.S. Noor-Soffalina, S. Jinap, S. Nazamid, S.A.H. Nazimah, Effect of polyphenol and pH on cocoa Maillard-related flavour precursors in a lipidic model system, Int. J. Food Sci. Technol. 44 (2009) 168–180.

[7] Comisión del Codex Alimentarius, Code of Practice for the Reduction of Acrylamide in Foods, France, 2009. http://www.fao.org/fao-who-codexalimentarius/codex-home/es/.

[8] FAO/WHO, Health Implications of Acrylamide in Food, Geneva, 2004.

[9] J. Oracz, E. Nebesny, D. Żyżelewicz, New trends in quantification of acrylamide in food products, Talanta 86 (2011) 23–34.

[10] M. Granvogl, P. Schieberle, Quantification of 3-aminopropionamide in cocoa, coffee and cereal products : CCCorrelation with acrylamide concentrations determined by an improved clean-up method for complex matrices, Eur. Food Res. Technol. 225 (2007) 857–863.

[11] E. Bermudo, E. Moyano, L. Puignou, M. Galceran, Liquid chromatography coupled to tandem mass spectrometry for the analysis of acrylamide in typical Spanish products, Talanta 76 (2008) 389–394.

[12] D.M.H. Farah, A.H. Zaibunnisa, Misnawi, Optimization of cocoa beans roasting process using response surface methodology based on concentration of pyrazine and acrylamide, Int. Food Res. J. 19 (2012) 1355–1359.

[13] M. Raters, R. Matissek, Acrylamide in cocoa: a survey of acrylamide levels in cocoa and cocoa products sourced from the German market, Eur. Food Res. Technol. 244 (2018) 1381–1388.

[14] S.I.F.S. Martins, W.M.F. Jongen, M.A.J.S. Van Boekel, A review of Maillard reaction in food and implications to kinetic modelling, Trends Food Sci. Technol. 11 (2000) 364–373.

[15] R. Jumnongpon, S. Chaiseri, P. Hongsprabhas, J.P. Healy, S.J. Meade, J.A. Gerrard, Cocoa protein crosslinking using Maillard chemistry, Food Chem. 134 (2012) 375–380.

[16] A.T. Bullock, G.M. Burnett, C.M.L. Kerr, Electron spin resonance spectra of radicals derived from acrylamide and methacrylamide, Eur. Polym. J. 7 (1971) 791–796.

[17] A. Chapiro, L. Perec, Polymerisation radiochimique de l'acrylamide dans des milieux de nature differente, Eur. Polym. J. 7 (1971) 1335–1355.

[18] M.J. Frisch, G.W. Trucks, H.B. Schlegel, G.E. Scuseria, M.A. Robb, J.R. Cheeseman, G. Scalmani, V. Barone, B. Mennucci, G.A. Petersson, H. Nakatsuji, M. Caricato, X. Li, H.P. Hratchian, A.F. Izmaylov, Gaussian. Revision A.1, Gaussian, Wallingford, CT, 2009. Bl, 09.

[19] R. Ditchfield, W.J. Hehre, J.a. Pople, Self consistent molecular orbital methods. IX. An extended Gaussian type basis for molecular orbital studies of organic molecules, J. Chem. Phys. 54 (1971) 724–728.

[20] J. Tomasi, B. Mennucci, R. Cammi, Quantum mechanical continuum solvation models, Chem. Rev. 105 (2005) 2999–3093.

[21] C. Wohlfarth, Fluid properties, in: CRC Handb. Chem. Phys., 85th ed., CRC Press, Boca Ratón, FL, 2005, pp. 981–1210.

[22] I.M. Alecu, J. Zheng, Y. Zhao, D.G. Truhlar, Computational thermochemistry: scale factor databases and scale factors for vibrational frequencies obtained from electronic model chemistries, J. Chem. Theor. Comput. 6 (2010) 2872–2887.

[23] Jeffrey P. Merrick, D. Moran, L. Radom, An evaluation of harmonic vibrational frequency scale factors, J. Phys. Chem. A. 111 (2007) 11683–11700.

[24] J.D. McQuarrie, D.A. Simon, Molecular Thermodynamics, Sausalito, CA, 1999.

[25] K. Fukui, Formulation of the reaction coordinate, J. Phys. Chem. 74 (1970) 4161–4163.

[26] K.B. Wiberg, Application of the pople-santry-segal CNDO method to the cyclopropylcarbinyl and cyclobutyl cation and to bicyclobutane, Tetrahedron 24 (1968) 1083–1096.

[27] A. Moyano, M. Pericas, E. Valenti, A theoretical study on the mechanism of the thermal and the acid-catalyzed decarboxylation of 2-oxetanones (beta.-lactones), J. Org. Chem. 54 (1989) 573–582.

[28] E. Glendening, A. Reed, J. Carpenter, NBO Version 3.1, 1988.

[29] S.W. Benson, in: The Foundations of Chemical Kinetics, first ed, McGraw-Hill, New York, 1969. https://archive.org/stream/foundationsofche033038mbp#page/n13/mode/1up.

[30] H. Glasstone, K.J. Laidler, K.J. Eyring, in: The Theory of Rate Processes, first ed., McGraw-Hill, New York, 1941. http://trove.nla.gov.au/version/25548457.

[31] M. Gil, Y. Jaramillo, C. Bedoya, S.M. Llano, V. Gallego, J. Quijano, J. Londono-Londono, Chemometric approaches for postharvest quality tracing of cocoa: an efficient method to distinguish plant material origin, Heliyon 5 (2019).

[32] Official Methods of Analysis of International, AOAC Moisture in Cacao Products, 2002.

[33] M. Gil, S. Llano, Y. Jaramillo, J. Quijano, J. Londono-Londono, Matrix effect on quantification of sugars and mannitol developed during the postharvest of cocoa: an alternative method for traceability of aroma precursors by liquid chromatography with an evaporative detector, J. Food Sci. Technol. (2019) 1–12.

[34] E.L. De Paola, G. Montevecchi, F. Masino, D. Garbini, M. Barbanera, A. Antonelli, Determination of acrylamide in dried fruits and edible seeds using QuEChERS extraction and LC separation with MS detection, Food Chem. 217 (2017) 191–195.

[35] F.A. Carey, R.J. Sundberg, Advance Organic Chemistry. Part A: Structure and Mechanisms, fifth ed., 2007. Berlin.

[36] F.A. Carey, R.J. Sundberg, Stereochemistry, conformation, and stereoselectivity, in: Adv. Org. Chem. Part A Struct. Mech., fifth ed., Springer, Berlin, 2007, pp. 119–251.

[37] G. Loaëc, P. Jacolot, C. Helou, C. Niquet-Léridon, F.J. Tessier, Acrylamide, 5-hydroxymethylfurfural and N(ε)-carboxymethyl-lysine in coffee substitutes and instant coffees, Food Addit. Contam. Part A. Chem. Anal. Control. Expo. Risk Assess. 31 (2014) 593–604.
[38] T. Kocadağlı, N. Göncüoğlu, A. Hamzalıoğlu, V. Gökmen, In depth study of acrylamide formation in coffee during roasting: role of sucrose decomposition and lipid oxidation, Food Funct. 3 (2012) 970–975.
[39] E. Vélez, P. Ruíz, J. Quijano, R. Notario, Gas-phase elimination reaction of ethyl (5-cyanomethyl-1,3,4-thiadiazol-2-yl)carbamate: a computational study, Int. J. Chem. Kinet. 48 (2015) 23–31.
[40] O. Smith, S. Cristol, Química Orgánica, fourth ed., 1970. Barcelona.
[41] S. Badui Dergal, in: Química de los alimentos, Cuarta, Pearson Educación de México, S.A. de C.V., Naucalpan de Juárez, México, 2006.
[42] O. Fenema, in: Química de los Alimentos, 2a ed., Winsconsi, 1993.
[43] J. Rodriguez-Campos, H.B. Escalona-Buendía, S.M. Contreras-Ramos, I. Orozco-Avila, E. Jaramillo-Flores, E. Lugo-Cervantes, Effect of fermentation time and drying temperature on volatile compounds in cocoa, Food Chem. 132 (2012) 277–288.
[44] D. Pacetti, E. Gil, N.G. Frega, L. Álvarez, P. Dueñas, P. Lucci, Acrylamide levels in selected Colombian foods, Food Addit. Contam. Part B Surveill. 8 (2015) 99–105.
[45] European Food Safety Authority (EFSA), Scientific Opinion on acrylamide in food 1, EFSA J 13 (2015) 1–321.
[46] European Food Safety Authority (EFSA), Acrylamide in food What is acrylamide? Why is it present in food? An overview of EFSA ' s risk assessment: what are the risks for consumers of acrylamide in food ? What happens to acrylamide in the body ? What is the margin of exposure ? Parma (2015).